Scattering of 200-Mev Positrons by Electrons*

J. A. POIRIER,† D. M. BERNSTEIN,‡ AND JEROME PINE

High-Energy Physics Laboratory, Stanford University, Stanford, California

(Received August 10, 1959)

Scattering of positrons by electrons has been investigated by bombarding a beryllium target with 200-Mev positrons and observing the recoil electrons in a diffusion cloud chamber located behind the target. The cloud chamber was in a magnetic field which permitted the yield of recoil electrons to be measured as a function of their energy W. The experiment covered the range $88 \leqslant W \leqslant 200$ Mev. The positron beam also traversed the cloud chamber and the total number of incident positrons was determined by track-counting.

The total electron yield for $88 \leqslant W \leqslant 200$ Mev is $(113 \pm 9)\%$ below that predicted by the first-order Bhabha theory. This difference cannot be interpreted until radiative corrections to the theory have been evaluated. A calculation of these corrections which is valid for the conditions of this experiment is not available. The shape of the electron energy spectrum is in good agreement with the Bhabha theory, and inconsistent with the theory if annihilation terms are omitted.

I. INTRODUCTION

BHABHA[1] has derived an expression for the scattering of positrons from electrons assuming the positron and electron are Dirac particle and antiparticle. The expression, which was derived in the first Born approximation, i.e., to first order in an expansion in terms of the fine structure constant $e^2/\hbar c = 1/137$, may be written

$$d\sigma(B) = d\sigma(R)\{D + I + A\},$$

where $d\sigma(R) = 2\pi r_0^2 [\beta^2(\gamma - 1)]^{-1}(d\epsilon/\epsilon^2)$ is the classical Rutherford cross section for $\gamma - 1 \ll 1$; $2\pi r_0^2 = 2\pi (e^2/mc^2)^2 = 0.50 \times 10^{-24}$ cm^2; $\beta = v/c$ for the incident positron; $\gamma = (1 - \beta^2)^{-\frac{1}{2}} = E_0/mc^2$; ϵ is the fraction of the incident positron's kinetic energy which is transferred to the electron, $(W - mc^2)/(E_0 - mc^2)$, where E_0 and W are the total energies of the incident positron and recoil electron, respectively;

$$D = 1 - \frac{\gamma^2 - 1}{\gamma^2}\epsilon + \frac{1}{2}\left(\frac{\gamma - 1}{\gamma}\right)^2\epsilon^2;$$

$$I = -\frac{\gamma - 1}{\gamma + 1}\left[\frac{\gamma + 2}{\gamma} - 2\frac{\gamma^2 - 1}{\gamma^2}\epsilon + \left(\frac{\gamma - 1}{\gamma}\right)^2\epsilon^2\right]\epsilon;$$

and

$$A = \left(\frac{\gamma - 1}{\gamma + 1}\right)^2\left[\frac{\gamma^2 + 2\gamma + 3}{2\gamma^2} - \left(\frac{\gamma - 1}{\gamma}\right)^2\epsilon(1 - \epsilon)\right]\epsilon^2.$$

The D term is due to direct scattering (charge plus Dirac magnetic moment); the A term is due to virtual annihilation; and the I term is due to the interference between D and A. All these quantities are expressed in the laboratory system.

To indicate the effect of the annihilation term and also the effect of the Dirac magnetic moment on the scattering, three cross sections have been plotted in Fig. 1. Curve I is the complete Bhabha cross section, and Curve II is the same theory without the annihilation terms I and A. Curve III is the cross section minus the magnetic moment and annihilation terms, i.e., the relativistic scattering of two distinguishable spin-zero Klein-Gordon particles $d\sigma(R)\{D'\}$. The Klein-Gordon cross section $d\sigma(K\text{-}G)$ including the annihilation terms is[2]

$$d\sigma(K\text{-}G) = d\sigma(R)\{D' + I' + A'\},$$

where

$$D' = 1 - \frac{\gamma - 1}{\gamma}\epsilon + \frac{1}{4}\left(\frac{\gamma - 1}{\gamma}\right)^2\epsilon^2,$$

$$I' = -\frac{(\gamma - 1)^2}{\gamma(\gamma + 1)}\left(1 - \frac{5\gamma - 1}{2\gamma}\epsilon + \frac{\gamma - 1}{\gamma}\epsilon^2\right)\epsilon,$$

$$A' = \left(\frac{\gamma - 1}{\gamma + 1}\right)^2\left(\frac{\gamma - 1}{\gamma}\right)^2(\epsilon^2 - \epsilon + \tfrac{1}{4})\epsilon^2.$$

The interpretation of these terms is analogous to that in the case of Bhabha scattering. It is interesting to note that in the extreme relativistic limit the sum of the terms above reduces to

$$D' + I' + A' = D + I + A = (1 - \epsilon + \epsilon^2)^2, \quad \gamma \gg 1,$$

so that the complete particle-antiparticle scattering in both theories (to first order in $e^2/\hbar c$) is the same.[3]

The cross sections above have been given in terms of ϵ, the fractional transfer of kinetic energy between incident positron and recoil electron in the laboratory system. The cross sections could also be expressed as angular distributions, since ϵ is uniquely determined by the scattering angle [$\epsilon = \sin^2(\theta/2)$, where θ is the scattering angle in the center-of-mass system]. The former functional dependence has been used for convenience;

---

† Now at the Lawrence Radiation Laboratory, University of California, Berkeley, California.

‡ Now at the Stanford Research Institute, Menlo Park, California.

[1] H. J. Bhabha, Proc. Roy. Soc. (London) A154, 195 (1936).

[2] M. Baker (private communication).

[3] This equality is also true in the case of identical particle scattering in the same limit.
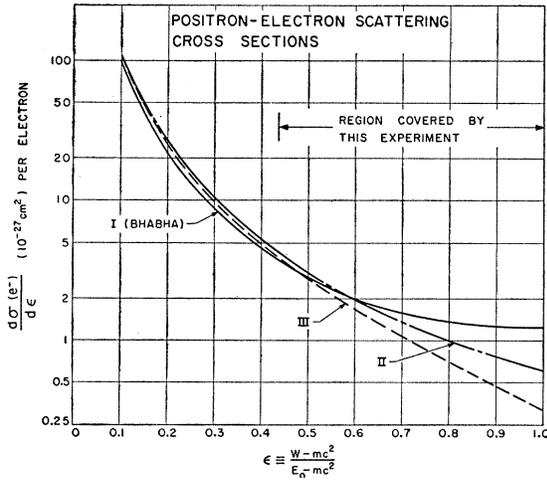
FIG. 1. The ordinate is the differential cross section for the scattering of a negative particle, initially at rest, which receives a final recoil kinetic energy of $(W-mc^2)$, where this energy has been expressed as a fraction of the incident kinetic energy (E_0-mc^2). Curve I is the complete Bhabha cross section and also the complete spin-zero Klein-Gordon cross section, II is the Bhabha cross section without annihilation terms, and III is the spin-zero Klein-Gordon cross section without annihilation terms. Curves are for $E_0=200$ Mev.

the range of ϵ in this experiment, $0.44 \leq \epsilon \leq 1.00$, corresponds to c.m. scattering angles $83° \leq \theta \leq 180°$.

Previous experiments on positron-electron scattering have utilized radioactive materials as positron sources, thus limiting the available positron energy to a few Mev. Several experiments have been performed with cloud chambers,[4-7] and more recent experiments have used counter techniques.[8,9] These experiments are consistent with the Bhabha cross section provided the annihilation terms are included. Our experiment was undertaken to check the Bhabha cross section at highly relativistic energies $(\gamma=395)$ and maximum transfer of momentum between the positron and electron. These conditions are of interest since effects such as radiative corrections, possible breakdown of quantum electrodynamics, and the finite size of positrons and electrons, become important at large momentum transfers in the center of mass, i.e., large 4-momentum transfers. However, for positrons at a laboratory energy of 200 Mev, the maximum 4-momentum transfer to a stationary electron is only about 14 Mev/c. For this 4-momentum transfer, Drell[10] has shown that the correction to the Bhabha cross section for the latter two effects is $\leq \frac{1}{4}\%$ if cancellations between effects of proton size, electron size, and the breakdown of

quantum electrodynamics do not invalidate limits obtained from electron-proton scattering experiments.[11]

This experiment measures only the energy spectrum of recoil electrons from positron-electron scattering and does not measure the inelasticity of the scattering events (see process B in Fig. 5). The consistent theoretical treatment of the elastic process (A in Fig. 5) is possible only to first order. The difference between this first-order treatment and a consistent second-order treatment, which must include processes of photon emission, is the radiative correction. This correction is a function of the maximum allowed photon energy k_{max}, which depends on the resolution of the experimental equipment. This experiment was analyzed in such a way that no limit was placed on k_{max} other than that resulting from over-all energy conservation, i.e., $k_{max} \doteq E_0(1-\epsilon)$. As a result of the wide limits on k_{max}, calculations of the radiative correction by Redhead[12] and Polovin[13] do not apply here. A calculation by Abrikosov[14] also does not apply since it assumes that the c.m. energy is much higher than that of this experiment. At present we know of no calculation which can be compared with the experimental results reported here. The most plausible interpretation of the comparison between the experimental results and the Bhabha theory is felt to be a measure of the radiative correction to positron-electron scattering in the limit of unrestricted k_{max}.

II. EXPERIMENTAL APPARATUS

A positron beam was produced from the high-energy electron beam of the Stanford Mark III linear accelerator.[15] The positrons were incident on a beryllium target placed immediately in front of a diffusion cloud chamber. The chamber was located in a magnetic field of about 5.5 kilogauss so that recoil electrons from the target could be momentum-analyzed. A scintillation counter placed behind the cloud chamber enabled the accelerator operator to monitor the positron beam and to maintain a predetermined optimum intensity.

The positrons were produced in a copper target of about $\frac{1}{2}$-radiation-length thickness placed near the midpoint of the accelerator. The 350-Mev electrons from the front part of the accelerator struck the target producing γ-rays by bremsstrahlung, which in turn produced the positrons in the remainder of the same target by the pair-production process. A schematic view of the accelerator showing the positron-production target and the location of the equipment is shown in Fig. 2. No rf power was fed to the part of the accelerator

[4] H. Zah-wei, Phys. Rev. 70, 224 (1946).
[5] O. Ritter et al., Z. Naturforsch 6a, 243 (1951).
[6] G. R. Hoke, Phys. Rev. 87, 285 (1952).
[7] R. R. Roy and L. Groven, Phil. Mag. 43, 1291 (1952).
[8] H. A. Howe and K. R. MacKenzie, Phys. Rev. 90, 678 (1953).
[9] Ashkin, Page, and Woodward, Phys. Rev. 94, 357 (1954).
[10] S. D. Drell, Ann. Phys. 4, 75 (1958).

[11] R. Hofstadter, Revs. Modern Phys. 28, 214 (1956).
[12] M. L. G. Redhead, Proc. Roy. Soc. (London) A220, 219 (1953).
[13] R. V. Polovin, J. Exptl. Theoret. Phys. U.S.S.R. 31, 449 (1956) [translation: Soviet Phys. JETP 4, 385 (1956)].
[14] A. A. Abrikosov, J. Exptl. Theoret. Phys. U.S.S.R. 30, 544 (1956) [translation: Soviet Phys. JETP 3, 379 (1956)].
[15] M. Chodorow et al., Rev. Sci. Instr. 26, 134 (1955).

FIG. 2. Plan view of experimental arrangement; M_D and M_F are deflecting magnets, Q_N and Q_S are quadrupole magnets. The copper radiator is the production target for the positrons.
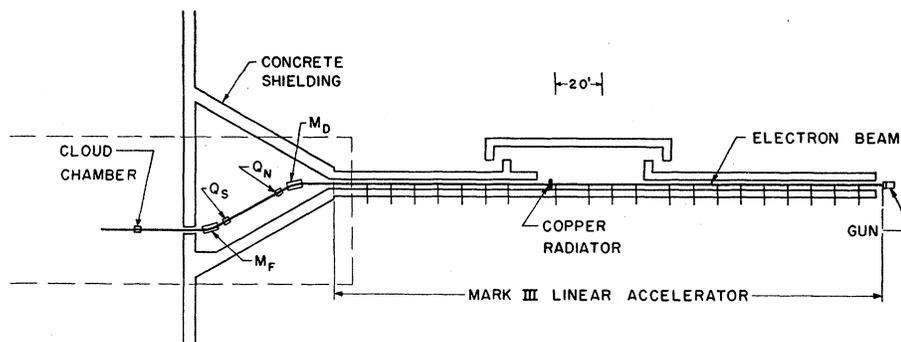
downstream of the production target so that positrons and electrons emerging from the target at small enough angles coasted to the entrance collimator of the magnet system at the end of the accelerator. The accelerator was pulsed once every 15 seconds.

Figure 3 illustrates the magnets and their focusing properties. The scale is distorted for clarity, the actual dimensions of the entrance collimator being $\frac{3}{16}$ in. high by $\frac{7}{8}$ in. wide. The deflecting magnet M_D and the energy slit select positrons with a momentum spread of $\pm 1\frac{1}{2}\%$ about the mean. The central momentum of this spectrum was determined to be (199 ± 1) Mev/c by floating-wire measurements. The π^+ and μ^+ content of the beam was negligible.

The over-all focusing properties of the magnet system were adjusted to produce a line beam, $\frac{1}{4}$ in. high and 10 in. wide, at the cloud chamber. This beam shape was

appropriate to the limited height and large width of the sensitive volume of the cloud chamber. The beam was in vacuum to within 10 in. of the beryllium target where it passed through a 0.008-in. Mylar window.

The beryllium target was (1.99 ± 0.01) g/cm^2 thick. A spectroscopic analysis of the target material showed various impurities totalling $\frac{1}{2}\%$ by weight. From these data the target is calculated to contain $(5.33\pm0.03) \times 10^{23}$ electrons/cm^2 and to have a thickness of 0.032 radiation length. In calculating the target thickness in units of radiation lengths, the effect of the atomic electrons in beryllium was accounted for by replacing Z^2 by $Z(Z+1.33)$.[16] The thickness in radiation lengths is involved only in the calculation of backgrounds and is given with sufficient accuracy by this expression.

The 18-in. $\times$ 24-in. diffusion cloud chamber[17] was operated at atmospheric pressure with a filling of

FIG. 3. An enlarged view of the section indicated in Fig. 2 by a dashed line. The top diagram is a view of the horizontal plane; the bottom diagram is a view of the vertical plane. The dimensions have been distorted to show the focusing properties of the magnetic lenses; M_D and M_F are $n=0$ deflecting magnets, Q_N and Q_S are quadrupole magnets, and PM is a scintillation counter.
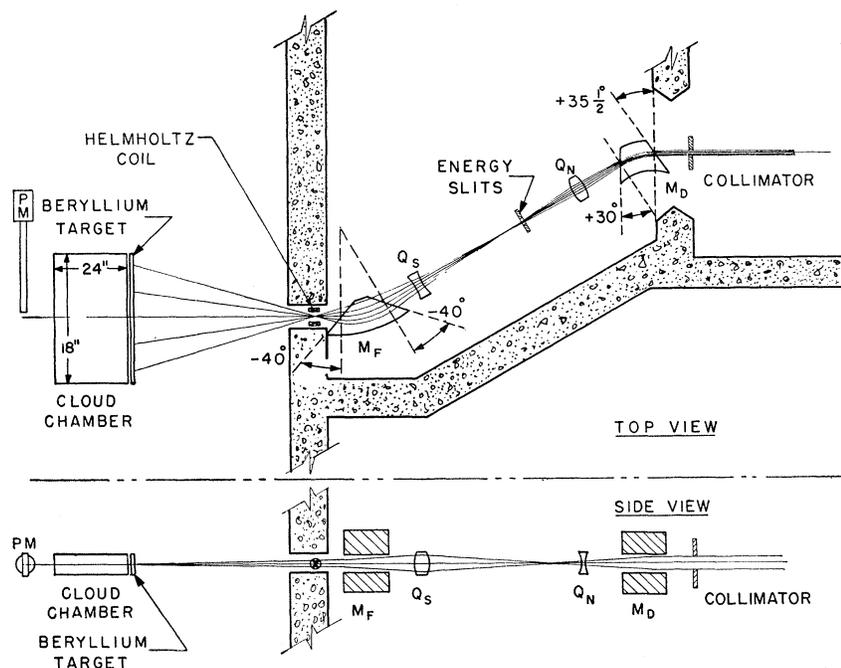
[16] H. A. Bethe and J. Ashkin, in *Experimental Nuclear Physics*, edited by E. Segrè (John Wiley and Sons, Inc., New York, 1953) Vol. 1, p. 263.
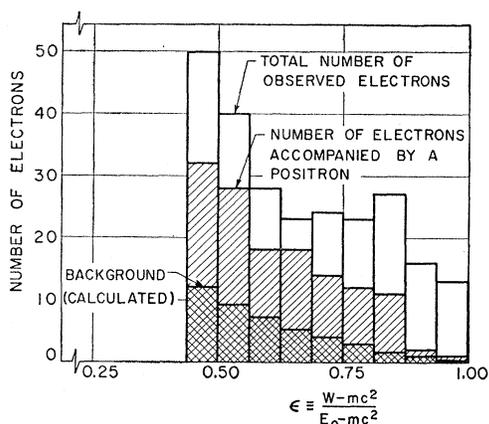[17] D. C. Hagerman and K. M. Crowe, Phys. Rev. **100**, 869 (1955).

FIG. 4. Observed electron spectrum (uncorrected data).

nitrogen gas and methyl alcohol vapor. The bottom of the cloud chamber was held at $(-40\pm\frac{1}{2})°C$ by a two-stage refrigerator. Stereoscopic pictures were taken from above the cloud chamber on Kodak 35-mm Tri-X film, the light flash occurring 0.19 sec after the arrival of the positron beam. After the cloud-chamber pictures were taken, the camera was fitted with a condenser point-source arc-light system which reprojected the developed images through the same lens system. By using the same lenses for camera and reprojector, lens distortions were cancelled to first order. The small effect of taking pictures through a $\frac{2}{3}$-in. plate-glass top of the chamber was compensated for by reprojecting through a similar piece of glass.

The magnetic field in which the cloud chamber was located was homogeneous to $\pm1.5\%$. The momentum measurements were not absolute; the curvature of the electron tracks was measured relative to the curvature of the incident positron tracks. The magnetic field inhomogeneity introduces no systematic errors since on the average the positrons and electrons see the same inhomogeneity. The spread in momentum measurements from this cause is included with other effects in Sec. IV. A, where the total spread was obtained from analyzing the distribution of measurements on the incident positron beam with the target removed.

III. EXPERIMENTAL RESULTS

The histogram in Fig. 4 shows the raw data obtained in the experiment. Recoil electrons were selected which originated from a region 6.6 in. wide in the center of the target. In this region the intensity of the incident positron beam was uniform and the beam was well focused vertically. In addition, the trajectories of both electrons and positrons from this region are far from the sides of the cloud chamber, resulting in optimum detection efficiency and measurability of the tracks. To obtain the number of positron-electron scattering events, two corrections to the raw data were necessary: first, the calculated background of electrons from other processes

was subtracted; and second, a correction was made for the fact that the efficiency for detecting recoil electrons from scattering events was less than 100%. The positron beam flux incident on this selected region of the target was measured so that the data define an absolute cross section.

A. Positron-Initiated Backgrounds

Figure 5 indicates some processes which could produce the electrons which were observed in the chamber. The processes A and B, elastic and inelastic positron-electron scattering, are the processes of interest; C, D, and E are positron-initiated background processes, and F, G, and H are the effects of possible contamination of the positron beam. No attempt was made to resolve A and B, and the experiment measures the sum of these two processes. The contributions of C (bremsstrahlung followed by pair production) and D (bremsstrahlung followed by Compton scattering) were calculated numerically. The intermediate-screening formulas of Bethe and Heitler were used for the bremsstrahlung[18] and pair-production[19] cross sections, and the Klein-Nishina formula[20] was used for the Compton scattering cross section. Two independent calculations of these cascade processes agreed to within 5%. Direct pair production by a positron, process E, was estimated to be 24% of C, independent of energy. This ratio of E/C was inferred from an experimental measurement by Camac.[21]

The background shown in Fig. 4 is that calculated for processes C, D, and E. Anticipating the discussion in Sec. C below, these background electrons are estimated to be detected with greater than 95% efficiency. This results from the fact that electrons from back-
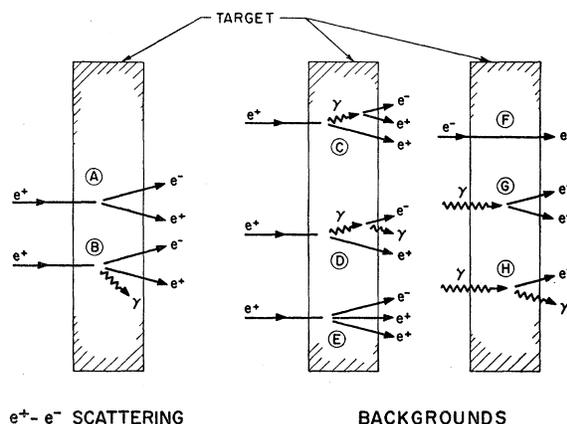

e^{+}- e^{-} SCATTERING   BACKGROUNDS

FIG. 5. Various processes which yield an electron: A and B are elastic and inelastic positron-electron scattering; C, D, and E are positron-initiated backgrounds; and F, G, and H are effects resulting from possible contamination of the positron beam.
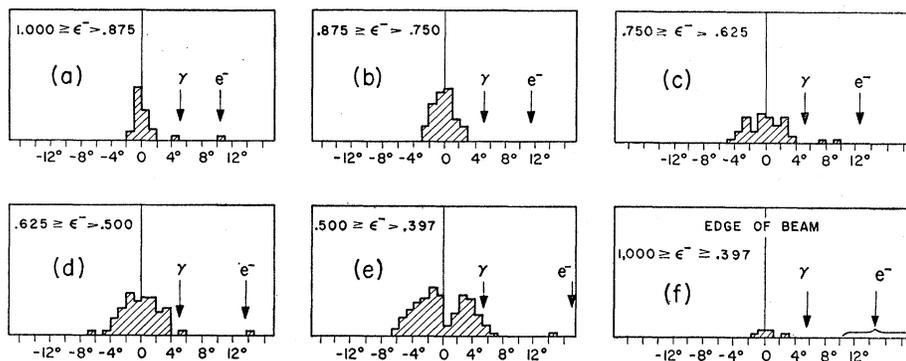
[18] Reference 16, p. 260.
[19] Reference 16, p. 327.
[20] Reference 16, p. 320.
[21] M. Camac, Phys. Rev. **88**, 745 (1952).

FIG. 6. Angular distribution of recoil electrons. The zero of these distributions is the measured direction of the incident positron beam at the target.

ground processes are produced at smaller angles than those from processes A and B. The maximum uncertainty in the background to be subtracted is estimated to be less than 10%, and the error in the final results from this uncertainty is negligible.

B. Possible Positron Beam Contamination

The following considerations place a limit of about 2% on the possible contribution of beam contamination (processes F, G, and H) to the observed electron yield, and indicate no positive evidence of any contamination: First, electrons and photons originating from the electron beam of the accelerator would have a spectrum of energies ranging up to 350 Mev, the energy of the electron beam incident on the copper positron production target. On the other hand, recoil electrons from the beryllium target that were scattered by the positron beam have a spectrum of energies up to only 201 Mev. In the entire chamber (which is two to three times the region used for data-taking) no negative tracks were seen with energies greater than 201 Mev that were within ±15° of the beam direction. The absence of electrons in this energy region indicates the absence of contamination particularly in the region of high recoil energies.

Secondly, the angle of the electron tracks after extrapolation back to the position of the Be target, relative to the direction of the incident positron beam, furnishes evidence of their origin. The fringing field of the magnet extends beyond the target, so that the positrons are deflected −4.5° before they strike the target; photon contamination will remain undeflected; and electron contamination will be deflected in the opposite direction by +(4.5/ε) degrees. The angle of possible contamination relative to the positron beam is defined to ±½° since the contamination is expected to pass through the same hole in the shielding wall as did the positron beam. The observed angular distributions of electron tracks at the target are presented in the first five histograms of Fig. 6; the zero of these distributions is the measured direction of the incident positron beam. The angle at which electrons from processes G and H would appear (+4.5°) is marked by

arrows labelled "γ"; similarly, the arrows marked "e^-" indicate the angle for electrons from process F. The cases which definitely look like effects of beam contamination can be quantitatively understood by considering the effect of the 0.008-in. Mylar window at the end of the beam vacuum pipe (outside the magnet fringing field) and the 10-in. of air between this window and the Be target. Processes A, B, and E in the Mylar appear as F contamination according to the angular criteria above; bremsstrahlung in the Mylar is a source of processes G and H. Processes originating in the air will occur at smaller angles. Ten of these "contamination" electrons are calculated to be observed in the cloud chamber. From the data in Fig. 6 any additional unexplained background is estimated to be $(0_{-0}{}^{+8})$ electrons, or $(0_{-0}{}^{+1.5})$% of the observed electron yield. The calculated background has been subtracted from the data so that comparisons of experiment with theory are based on processes taking place only in the Be target.

Thirdly, a similar angular analysis at the edge of the positron beam was performed. In this region the intensity of incident positrons is greatly reduced, yet contamination, which is not expected to be focused by the magnet system, should be at full intensity. (Also, electrons from positron-initiated events in the Mylar cannot appear in this region.) If the effect of contamination amounted to 2% of the observed electron yield, then the probability is only 0.23 that no contaminant tracks would be found, which is the case as shown in Fig. 6(f).

These considerations are felt sufficient to show that the electron yield from possible beam contamination was less than 2% of the yield from positron-electron scattering events.

C. Detection Efficiency

The possibility that an electron track might be missed during scanning was minimized by a re-scan of 67% of the pictures. On the basis of one missed electron track by one scanner in half this group of doubly-scanned pictures, about 0.5 track is predicted to be missed in the entire electron search, which introduces a negligible correction.
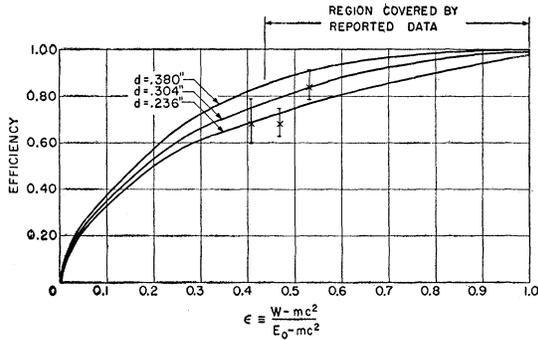
FIG. 7. Efficiency for observing electrons.

A more important factor influencing the detection efficiency is the possibility that the electron emerges from the target so as to leave the sensitive volume of the cloud chamber before it reaches a required minimum distance from the target. In the cloud chamber photographs the region of view begins 2.6 in. from the target. However, in order to provide sufficient track length for useful measurements, it was required that acceptable electron tracks stay within the region of the active volume for a minimum distance of 5.1 in. from the target. The probability that an electron fails to fulfill this requirement has been calculated. The calculation depends upon the height of the sensitive volume of the cloud chamber, the vertical distribution of the incident beam, multiple Coulomb scattering of the incident positrons and recoil electrons in the target, and the positron-electron scattering angle. The latter two are known functions of electron energy.

The beam height distribution was measured utilizing the two stereoscopic views of the cloud chamber; the measured distribution was approximately Gaussian in shape with a full width at half-maximum of 0.28 in. The efficiency calculation is particularly sensitive to a parameter d, the distance of the center of the beam from the top of the active volume. Figure 7 shows the calculated detection efficiency as a function of ϵ for three values of d. A measurement of d was obtained from additional pictures taken during the cloud-chamber run while the beam was raised and lowered by means of Helmholtz coils 20 ft from the cloud chamber. These pictures were taken between groups of about 1000 data pictures. The average value of d obtained from an analysis of these pictures was (0.38 ± 0.07) in. and the sensitive volume was found to be 1.1 in. high. This measurement of d, together with the calculation, defines the efficiency as a function of ϵ.

In addition, a direct determination of the efficiency for ϵ near 0.5 was obtained by considering the number of electrons accompanied by a scattered positron in comparison with those that were not. A positron "accompanies" an electron if it is judged to come from the same event, i.e., if its extrapolated origin in the

target is within 0.5 cm of the electron's origin and its energy is $\leq (E_0 - W)$.

The positron-electron scattering events at a given ϵ may be classified into groups A, U^+, U^- and N, where in A, both e^+ and e^- are observed; in U^+, e^+ is observed but not e^-; in U^-, e^- is observed but not e^+; and in N, neither e^- nor e^+ is observed. The efficiency η for detecting the recoil electron is given by

$$\eta = (A + U^-)/(A + U^- + U^+ + N).$$

In practice, U^+ is indistinguishable from the many positrons of energy less than 200 Mev which result from radiative straggling of the incident beam. There exists, however, an electron energy ($\epsilon \doteq 0.5$) such that the recoil electrons and scattered positrons have identical energies and angles. At this energy $U^- = U^+$, so that $\eta = (A + U^-)/(A + 2U^-)$ if N is negligible. It is calculated that N has a probability of ≤ 0.005 at $\epsilon \doteq 0.5$. This probability is small due to the coplanarity of the positron and electron in the scattering process, which leads to a high probability of one particle being observed if the other is not. (Since the incident beam is above the center of the sensitive volume, scattering upwards is almost always the cause of a particle not being seen.) Thus the efficiency at this energy can be obtained from the number of observed accompanied and unaccompanied electrons. Various energy degradation processes tend to lower the value of this symmetrical energy below $\epsilon = 0.5$ to a value indicated by the middle experimental point of Fig. 7. The other two points were obtained from a straightforward extension of this symmetry argument which applies to data for ϵ above and below the symmetrical energy.
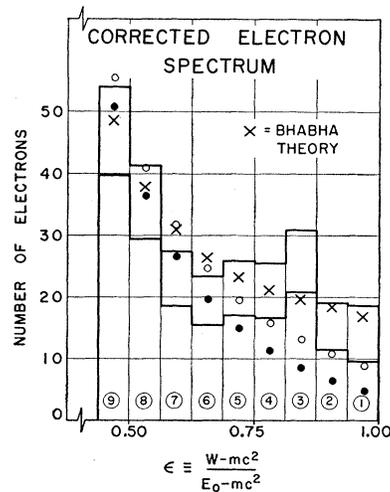
Each of these experimental points can be used to

FIG. 8. Comparison of the experimental yield of electrons with predicted yields: cross, Bhabha theory; circle, Bhabha theory with annihilation terms omitted; solid circle, Klein-Gordon theory with annihilation terms omitted. The corrected experimental yield for each bin is indicated by an upper and a lower bar which show limits of plus and minus one standard deviation from the best experimental value.

define (by means of the efficiency calculation) a value of d with corresponding uncertainties. Combining the three values yields $d=(0.26\pm0.06)$ in. This in turn was combined with the directly measured value of $d=(0.38\pm0.07)$ in. to obtain the final result $d=(0.31\pm0.06)$ in. The efficiency which was used to correct the observed electron yields was defined by the calculated efficiency assuming this latter value of d (the error limits on d define the uncertainty introduced by the efficiency correction).

Estimates have been made of possible systematic errors in the direct d measurement or in the indirect measurement (from the direct efficiency determination). No significant effects were found, but the possibility of systematic errors has led to the error assignment ±0.06 in. for d even though the usual statistical treatment would indicate a smaller error.

The final experimental results for the electron yield from positron-electron scattering events in the Be target are indicated in Fig. 8 by an upper and lower line in each energy bin which indicate limits of plus and minus one standard deviation based on the statistical error combined with the uncertainty in the efficiency correction. Other errors are negligible in comparison with these. In addition to the background and detection efficiency corrections discussed previously, the electron yield in the highest-energy bin has been increased by 10.7%. This corrects for the fact that the momentum limits of this bin were defined in such a manner that energy loss by ionization narrowed the bin width. The smaller effect of ionization loss for the other bins is discussed in the next section and is one of the corrections applied to theory before comparison with the experiment.

The total experimental yield of electrons from positron-electron scattering with fractional electron energies ϵ between 0.44 and 1.00 is 216 ± 21. The error (estimated standard deviation) is composed of: counting statistics, $\pm8.1\%$; efficiency correction uncertainty, $(+4.7, -3.0)\%$; electron scanning inefficiency, $(+0.8, -0.0)\%$; possible beam contamination, $(+0, -2)\%$; uncertainty in the subtracted background, $\pm2\%$.

D. Total Positron Flux

The total positron flux incident on the target in the region from which recoil electron events were analyzed was obtained by directly counting the positron tracks. Since the number of positrons per picture was kept approximately constant, only a small sample (about 4%) of the pictures was track-counted, and the average count per picture obtained from these 415 pictures was then extended to the total number (10 248) of analyzed pictures. Care was taken that the 415 pictures were randomly selected from the data pictures. Uncertainties which result from this procedure are due to scanning errors and statistical errors.

The scanning error was investigated by establishing

TABLE I. Scanning efficiency.

| | Scanners | | |
	A	B	C
Systematic error	−0.5%	−2.4%	−0.4%
Percent of the pictures analyzed	74%	85%	13%
Corrected subtotals for data pictures scanned twice	2293		2290
	10 100	10 122	
		552	558

a standard "true" count for a representative sample of data pictures which were used as test pictures. Each scanner's total per test picture was then compared with the standard to establish his systematic error; the results are shown in Table I. The standard was established by having several people separately scan the test pictures and then resolving the differences in a collective re-scan. Those differences which remained unresolved amounted to $\frac{1}{2}\%$ of the total number of tracks, so that the standard is believed to be accurate to about $\pm\frac{1}{2}\%$. A check of the systematic error assignments obtained from the test pictures is available from the 67% of the data pictures that were counted by more than one scanner. If each scanner's results are corrected for his inefficiency as obtained from the test pictures, then the subtotals for data pictures scanned twice are in good agreement, as is seen in Table I.

The statistical error in extending the average number of tracks per picture (44.5) obtained from $\sim4\%$ of the pictures to the total number of pictures, amounts to 1.5%. This error was evaluated from the measured distribution of track counts per individual picture. This measured distribution was about 70% broader than that to be expected purely from Poisson statistics, presumably as a result of fluctuations in accelerator operating conditions. The final result for the number of positrons incident on the target in the region from which data were accepted is $(4.56\pm0.07)\times10^5$. The quoted error is dominated by the statistical error.

IV. COMPARISON WITH THEORY

Ideally, the expected yield of electrons $Y(\Delta W)$ in an energy interval ΔW extending from W_1 to W_2 is given by

$$Y(\Delta W)=X_eN\int_{W_1}^{W_2}d\sigma(E_0,W),\qquad(1)$$

where X_e, the thickness of the target in electrons/cm^2, is $(5.33\pm0.03)\times10^{23}$; N, the total number of incident positrons, is $(4.56\pm0.07)\times10^5$; and $d\sigma$ is the theoretical differential cross section per electron for producing a recoil electron of energy W by the scattering of a positron of energy E_0.

A. Experimental Corrections to Theory

The yield calculated from Eq. (1) must be corrected before it is compared with data. The most important

TABLE II. Corrections to Bhabha theory.

	1	2	3	4	5	6	7	8	9	Total
					Bins					
Electron energy interval	$\epsilon \leq 1.000$ $\epsilon \geq 0.9375$	≤ 0.9375 ≥ 0.8750	≤ 0.8750 ≥ 0.8125	≤ 0.8125 ≥ 0.7500	≤ 0.7500 ≥ 0.6875	≤ 0.6875 ≥ 0.6250	≤ 0.6250 ≥ 0.5625	≤ 0.5625 ≥ 0.5000	≤ 0.5000 ≥ 0.4375	≤ 1.000 ≥ 0.4375
Uncorrected yield (electrons)	19.7	20.1	20.8	22.2	24.3	27.4	32.2	39.4	50.8	256.9
Bremsstrahlung (%)	−15.2	−9.0	−6.6	−5.3	−4.1	−3.4	−2.9	−2.7	−2.5	−4.9
Ionization (%)	−0.1	−0.3	−0.5	−0.8	−1.1	−1.5	−1.9	−2.5	−3.0	−1.6
Momentum (%)	+0.3	+0.4	+0.6	+0.8	+1.0	+1.2	+1.5	+1.7	+2.1	+1.3
Total correction to theory (%)	−15.0	−8.9	−6.5	−5.3	−4.2	−3.7	−3.3	−3.5	−3.4	−5.3
Corrected yield (electrons)	16.8	18.3	19.5	21.0	23.2	26.4	31.1	38.1	49.0	243.4

effects are the energy degradation of incident positrons and recoil electrons by bremsstrahlung and ionization within the target, the uncertainty in determining the momentum of the recoil electrons, and the spread in energy of the incident positron beam.

The last effect was reduced by utilizing the fact that the energy of the incident positrons was correlated with their position across the target. The events were analyzed in three groups, for each of which the spread in incident energy was ±0.5%. This spread, and the uncertainty of ±0.6% in the value of the mean energy of the positron beam, are of negligible importance.

The most important correction is that for energy loss by bremsstrahlung. A corrected cross section $d\sigma_c(E_0,W)$, to be used in place of $d\sigma(E_0,W)$ in Eq. (1), is given by

$$d\sigma_c(E_0,W) = \int \int \int P(E_0 \to E_0', x)dE_0'$$

$$\times d\sigma(E_0',W')dxP(W' \to W, x)dW', \quad (2)$$

where $P(E_0 \to E_0', x)dE_0'$ is the probability of an incident energy E_0 being degraded to E_0' by bremsstrahlung before a scattering event which takes place at x, the fractional distance through the target; $d\sigma(E_0',W')$ is the theoretical scattering cross section; and $P(W' \to W, x)dW'$ is the probability that the energy W' of the recoiling electron will be degraded to W in the remainder of the target. The percentage difference obtained by using the corrected Bhabha cross section obtained from Eq. (2) in the integral of (1) rather than the uncorrected Bhabha cross section is listed in Table II in the row labelled "Bremsstrahlung." The integral in Eq. (2) was evaluated assuming that multiple photon emission is negligible. This is justified because the target is relatively thin and very small energy losses are not important. It was possible to evaluate analytically the correction $(d\sigma_c - d\sigma)$ for $d\sigma$ equal to the Bhabha cross section and the probability of radiative straggling derived from a bremsstrahlung cross section proportional to dk/k, where k is the photon energy. This result was corrected by a calcu-

lation using the correct bremsstrahlung spectrum and approximating the Bhabha cross section. By this procedure, $(d\sigma_c - d\sigma)$ can be obtained to good accuracy.

The cross section has been corrected for the effect of energy loss by ionization using a procedure similar to that used for the bremsstrahlung correction. A uniform rate of energy loss of 1.33 Mev per g/cm² was assumed. The correction is listed in the row labelled "Ionization" in Table II. (The first-order effect which shifts the end-point of the spectrum was applied as a correction to the experimental yield in the highest-energy bin, as mentioned earlier.)

Momentum measurement errors were of two types, systematic and random. The films were projected onto a fixed plane, resulting in an error in the radius of curvature essentially proportional to the average vertical track displacement. This causes a random and a systematic error due to the fact that the positron beam was near the top of the active volume, and, of the electrons seen, more were scattered downward than upward. These errors, most important for low ϵ, were calculated from the known angular distribution of scattered electrons. Other random errors in momentum measurement were directly evaluated by measuring the radius of curvature of monoenergetic incident positron tracks in pictures taken with the target removed. These errors were found to be less than or equal to ±1%. The various momentum errors yield the corrections listed in Table II in the row labelled "Momentum."

The Bhabha theoretical yield, corrected for experimental effects, is indicated in Fig. 8 by crosses for each energy bin. The predicted yields for the Bhabha theory minus annihilation terms and the Klein-Gordon theory minus annihilation terms have also been indicated with their appropriate corrections.

B. Comparison of Experiment with Theory

The experimental energy spectrum has been compared with theoretical predictions by means of the χ^2 test. The P-value which results from this test is interpreted as the probability that a repetition of the observations would show greater statistical deviations (than those

TABLE III. χ^2 test for goodness of fit listing the resulting P values, i.e., the probability that a repetition of this experiment would show equal or greater statistical deviations from the assumed theory than those which were observed.

	Complete Bhabha theory	Bhabha theory minus annihilation terms	Klein-Gordon theory minus annihilation terms
High experiment	0.62	0.02	$<e^{-25}$
Best experiment	0.50	0.02	$<e^{-24}$
Low experiment	0.33	0.02	$<e^{-23}$

observed) from the theory which is assumed to govern the data. The analysis is complicated by the fact that part of the experimental error is statistical and part is systematic (as a result of the uncertainty in the efficiency determination). Therefore the χ^2 test was performed for the statistically independent deviations as a function of the systematic deviation. The probabilities labelled "High Experiment" in Table III are the result of the χ^2 test as applied to the experimental points corrected for an efficiency which is too low by one standard deviation (as defined by a value of the parameter d which is one standard deviation too low). Correspondingly, "Best Experiment" refers to the adopted efficiency, and "Low Experiment" to a value of the efficiency which is one standard deviation too high.

The integrated yield of electrons for ϵ between 0.44 and 1.00 which is predicted by the Bhabha theory corrected for the effects listed in Table II is (243 ± 5)

electrons; the error consists of uncertainties of $\pm0.5\%$ in the target density, $\pm1.1\%$ in the corrections listed in Table II, and $\pm1.5\%$ in the incident positron flux. This is to be compared with the experimental yield of (212 ± 21) electrons.

C. Discussion

The probabilities in Table III show that the measured spectrum is in reasonable agreement with the Bhabha theory and discriminates quite well between this and theories which neglect annihilation and spin.

If the difference in integrated theoretical and experimental yields is ascribed to radiative corrections, then this correction to the Bhabha theory is $(-13\pm9)\%$ averaged over recoil electron fractional energies in the range $0.44\leq\epsilon\leq1.00$, for 198-Mev incident positrons. The experimental analysis has been carried out in such a fashion that no restriction is placed on the energy of photons emitted in the scattering process. Nothing can be said of other possible effects until a calculation of the radiative corrections is available.